MINISTRY OF SUPPLY

AERONAUTICAL   RESEARCH   COUNCIL

CURRENT   PAPERS

An Analysis of the Air Flow through the Nozzle Blades of a Single Stage Turbine

By

I. H. Johnston

NATIONAL GAS TURBINE ESTABLISHMENT

An Analysis of the Air Flow through the
Nozzle Blades of a Single Stage Turbine

- by -

I.H. Johnston.

SUMMARY

This memo. presents the results of detailed traverses made on three

of the nozzle assemblies designed for a single stage experimental turbine.

The effects of pitch/chord ratio on gas outlet angle and total head loss are

recorded and discussed in the light of corresponding work published else-

where.   The value of pitch/chord ratio giving minimum total head loss is

found to compare well with the optimum pitching given by two dimensional

results obtained from cascade tests on blades of a similar nature.

CONTENTS

ILLUSTRATIONS

1.0 Introduction

The three nozzle assemblies used in this investigation are all composed of the same type of blading, the only difference being in the number of blades per row, i.e. pitch/chord ratio.

This note, which records the first part of a series of tests to determine the importance of blade pitching on turbine performance, is aimed first at determining optimum S/C for a nozzle row, and second at providing data regarding total pressure losses and flow patterns for the nozzles tested.

An attempt is made to analyse the results with regard to the following points.

1. Comparison of axial and swirl velocity distributions with those required by conditions of radial equilibrium.

2. Comparison of gas outlet angles with those corresponding to the simple $\cos^{-1} {}^{o}\!/_{s}$ rule (viz: outlet flow angle = $\cos^{-1} {}^{o}\!/_{s}$).

3. Comparison of total head loss with the results of cascade tests.

2.0 Blade Details

The blade profile, which was the same for all S/C's is shown in Fig. 2.

It is built up from circular arcs and has zero inlet blade angle and an outlet blade angle of 65.75°. Both blade chord and stagger are constant at all blade heights, the chord being 1.33" and the stagger angle equal to 41°. The blade spacings tested were:- Case (1) 36 blades, mean S/C = 0.739, Case (2) 27 blades, mean S/C = 0.985; Case (3) 22 blades, mean S/C = 1.208.

3.0 Apparatus, Instrumentation and Test Procedure

3.1 Apparatus

A general layout of the turbine casing and traversing gear is shown in Fig. 1. The turbine inlet volute consists of a tapering pipe which encircles the turbine and from which the air passes to the inlet annulus via eight radial passages.

3.2 Instrumentation

(a) Inlet: Four static tappings and four pitot tubes are located around the annulus. The pitots are enclosed in streamlined shields which also house thermocouples at three different radii.

(b) Outlet: Four statics are set in the outer wall and in the same plane there is a three-pronged static probe which is used to explore the static pressure gradient. A further four statics are set in the exhaust cone of the turbine, the common connection from these tappings being led out through one of the support spiders.

(c) Traversing gear: The traversing gear which was constructed for these tests is shown in Fig. 1. It has three principle components: the disc which occupies the position of the turbine rotor and from which protrudes the pitot yawmeter, the shaft which runs in the turbine bearings and in which the concentric control rods of the traversing mechanism are carried, and the cage which houses the two control wheels with their smaller recording discs.

The wheel farthest from the turbine casing is clamped to the central spindle which controls the radial position of the pitot tube while the other wheel determines the yaw of the instrument. Circumferential movement is

over the entire 360°, the angular position being fixed by a ratchet system
which provides for movement in steps of down to 1°. The pitot yawmeter was
manufactured from millimetre tubing and is of 'L' form with chamfered yaw
tubes.

Also located in the traversing gear disc are four static tappings which
are equally spaced around the rim.

(d) Air flow: The air flow through the turbine volute was controlled by
a throttle valve situated in the ducting leading from the main air supply
compressor.

4.0 Procedure

Throughout the tests the mass flow was maintained substantially con-
stant. This resulted in an outlet Mach number range of from 0.70 in case
1 to 0.40 in case 3 but for this type of blading it is reasonable to assume
that flow conditions are unaffected by this range of Mach number (c.f. Ref.1).

The corresponding Reynolds numbers based on blade chord and outlet
velocity ranged from 4.60 x 10⁵ in case 1 to 2.60 x 10⁵ in case 3.

4.1 Inlet Traverse

The inlet annulus was traversed to determine the velocity profiles,
both circumferential and radial, at entry to the nozzles. For a number of
radii readings of ΔP, the difference between the total head measured by the
fixed instrument and that indicated by the traversing pitot, were taken at
3° intervals round the annulus and these are plotted in terms of $\Delta P / \frac{1}{2} \rho V_1^2$

in Fig. 3, V_1 being the velocity as measured at the inlet pitots.

In the curves of Fig. 3, the wakes from the pitot/thermocouple instru-
ments are clearly defined but they affect only a small proportion of the
annulus cross section. The variations of total head over the annulus apart
from the boundary layer regions and the aforesaid wakes are all within about
± 4% of the mean dynamic head.

4.2 Nozzle Traverses

The nozzle traversing was restricted to the investigation of flow
behind two adjacent blade passages and at this stage the choice of the L-type
pitot yawmeter proved troublesome as it could not be yawed without a result-
ant alteration in the position of the open end of the pitot tube. The
instrument was accordingly calibrated in terms of yaw difference and total
head, the datum yaw being set by lining up a 3 ft. pipe of approximately $\frac{1}{2}$"
bore parallel to the shaft of the traversing gear to ensure true axial direc-
tion. All yaw readings may be subject to an error of up to $\pm \frac{1}{2}°$ due to a
small degree of back lash in the gear mechanism.

In order that the loss distribution should be determined as accurately
as possible the circumferential shift of the air from the leading edge of the
nozzle to the open end of the pitot tube was approximately evaluated and
taken into account during the computation.

4.3 Method of Plotting Results

In all cases where variation of loss is plotted against blade height the
circumferential mean values for each radius are taken. These were obtained
by graphical integration of the circumferential traverses so that for any
radius r:-

$$\Delta P = \left. r \int_{\theta_1}^{\theta_2} \delta P \, d\theta \middle/ r \int_{\theta_1}^{\theta_2} d\theta \right.$$

where δP is the local change in total head at any given radius and θ_1 and θ_2 are the limits of the traverse arc.

In obtaining the overall total head loss for each nozzle the area mean value was also calculated by graphical integration.

$$\overline{\Delta P} = \left. \int_{r_1}^{r_2} 2 \pi r \, \Delta P \, dr \middle/ \pi (r_2^2 - r_1^2) \right.$$

where r_1 and r_2 are the inner and outer radii.

5.0   Presentation and Analysis of Results

5.1   Inlet Velocity Distribution

In Fig. 4a the inlet velocity is plotted in the form $V_a/\overline{V}_a$ against r where V_a is the circumferential mean at each radius and $\overline{V}_a$ is the area mean velocity entering the nozzles. This area mean velocity equals $0.97 \, V_1$ where V_1 is the velocity measured at the inlet pitots.

Expressed in another form we have

$$\overline{P_1 - P_{stat_1}} = 0.943 \times (P_{INSTRUMENT} - P_{stat_1})$$

5.2   Radial Distributions of Outlet Velocity

The distributions of total gas outlet velocity are shown in Fig. 4a and comparison with the inlet distribution shows that whereas the boundary layer at the outer wall appears unchanged, the boundary layer next to the inner wall increases in thickness during its passage through the nozzle row.

The irregularity near the outer wall in case 3 can be attributed to breakaway which, as will be shown later, occurs over the outer half of the blades on this nozzle row.

The radial distributions of axial and swirl velocities are shown in Figs. 4b and 5a and may be compared with those required to give radial equilibrium for the observed total heads and gas outlet angles. Also, shown are what might be termed the 'ideal' velocity distributions, which give radial equilibrium for an angle distribution according to the $\cos^{-1} O/S$ rule and for the assumption of constant total head along the blade height. Comparison of the observed velocities with those giving radial equilibrium gives good agreement over most of the annulus height - apart from the region of flow close to the inner wall where the low velocities can be attributed to the thickening boundary layer. Considering the axial velocity profile of case 1 there are two regions of high velocity. As S/C increases, the high velocity region near the outer wall is maintained but tends to widen and move inwards, but the high velocity near the inner wall disappears in

cases 2 and 3.   Now, high axial velocities correspond to low outlet angles, thus as S/C is increased the gas angles in the outer part of the annulus decrease relative to mean diameter conditions and the angles near the inner wall increase.

5.3   Radial Distribution of Gas Outlet Angle

The outlet angle distributions are shown in Fig. 5b together with the three cos $^{-1}$ O/S distributions and, considering the limits of accuracy, the observed angles at mean diameter agree closely with the values obtained by the cos $^{-1}$ rule.   There is, however, a marked falling-off in outlet angle in the outer half of the annulus, this effect increasing with S/C.

At first sight this decrease in angle might be attributed to breakaway from the upper surfaces of the nozzle blades, but inspection of the loss contours and loss distributions (Fig. 6a) reveals that case 3 is the only one in which marked separation is occuring.

When considering these outlet angles it is advisable to bear in mind the secondary flows existing in the system.   These flows and their effects have been established and described in some detail in Refs. 7 and 8 and are represented pictorially in Fig. 6b.   This sketch shows the secondary flows which originate in a blade passage together with the vortices which are shed near each end of the trailing edge of a blade, and the resultant gas outlet angles can be compared with the cos $^{-1}$ O/S distribution.   Returning to Fig. 5b we see that these secondary flow effects are clearly in evidence near the outer wall, but do not appear at the inner wall, also that the effects seem to increase with S/C.   This increase with S/C is not unexpected as it is generally accepted that the secondary flows vary with the circulation at mean blade height which for comparable deflections increases with blade pitching.

Tests made by Lyth (Ref. 6) on the nozzles of the W2/500 turbine show a similar distribution of outlet angle near the outer wall.

American work on this subject, reported in Ref. 4 and 5 has produced somewhat different results.   For nozzles of similar blade form an outlet angle distribution is recorded in which there are little or no secondary effects at the outer wall, but very high outlet angles near the inner wall. These are attributed to a thick layer of 'dead' flow indicated by total head traverses near the inner wall.   As, however, no inlet traverses are recorded it is impossible to say whether this thick retarded layer is a result of faulty inlet design or that it is caused by reduced blade spacing, the S/C being 0.66 in the American tests as compared with 0.739 in case 1.

Further tests with the present rig on a nozzle row of small S/C will be necessary before any useful comparison can be made between the two sets of results.

The momentum mean outlet angle, related to the mean diameter, was evaluated for each blade spacing.   These mean outlet angles were 62.7°, 59.1° and 52.8° for cases 1, 2 and 3 respectively.

5.4   Radial Distributions of Total Head Loss

The total head losses across each nozzle row are shown in the form of contours in Figs. 7, 8 and 9.   The apparent off-set line of the wakes is due to the radial variation of outlet angle and in Fig. 9 it is interesting to note the increase in width of the wake at the region of breakaway.   The influence of the secondary flows in reducing this separation near the outer wall is also noticeable.

In Fig. 6a the radial distributions of circumferential mean loss are shown and again the separation over the outer half of the blades of case 3 is clearly indicated.

From these results the area mean of total head loss for each row was calculated and the resultant values are shown in Fig. 10 plotted against S/C from which curve it can be seen that the S/C for minimum loss is approximately 0.9.

Shown also in Fig. 10 is the variation in profile loss for this type of blading obtained from the general performance curves for turbine nozzles produced by Ainley in Ref. 2. It is interesting to note that the S/C for minimum profile loss coincides with that giving minimum total head loss.

Applying the approximations for secondary losses and annulus loss suggested in Ref. 2, good agreement is found in cases 1 and 3 but the empirical rules fail for the intermediate S/C's and they indicate an S/C for minimum loss which is much below the observed value.

Finally, although Bridle (Ref. 1) has shown that for a wide range of turbine blades there is little or no change in profile loss with Mach No., the results presented here can only be assumed valid for the Mach number range considered.

Further tests will be required to determine the variation of total head loss with Mach number.

6.0   Conclusions

1.   The distribution of axial velocity around the inlet to the turbine nozzles is tolerably uniform and suffers little interference from the inlet instruments.

2.   The axial velocity leaving the nozzles is comparatively uniform over most of the blade height for the three values of S/C.

3.   The agreement between observed axial and swirl velocities and those based on radial equilibrium requirements is fair over most of the annulus height apart from regions close to the walls.

4.   The S/C for minimum total head loss is approximately 0.9 which agrees with the corresponding figure for cascade tests on blades of similar profile.

5.   The mean outlet angles for the three S/C's based on equivalent angular momentum are:-

Row	1	2	3
S/C	.739	.985	1.208
α_2	62.7	59.1	52.8

6.   The area mean values of total head loss are:-

Row	1	2	3
S/C	.739	.985	1.208
$\dfrac{\overline{\Delta P}}{\overline{P}_2 - P_{stat_2}}$	0.0612	0.0556	0.114

REFERENCES

No.	Author(s)	Title etc.
1	E.A. Bridle	"Some high speed tests on turbine cascades". N.G.T.E. Report No. R.48. (A.R.C. 12,455 EA134)
2	D.G. Ainley	"An approximate method for the estimation of the design point efficiency of axial flow turbines". A.R.C. Current Paper No. 30. (A.R.C. 12,884 EA148)
3	A.D.S. Carter	"Vortex wind tunnel tests on various vortex flows". P.J. Report No. R.1063.
4	M.C. Huppart & C. Mac Gregor	"Comparison between predicted and observed performance of gas turbine stator blade designed for free vortex flow". N.A.C.A. Tech. note 1810.
5	A.W. Goldstein	"Aerodynamic and matching characteristics of turbine component determined with cold air". N.A.C.A. Report 878.
6	M. Lyth	"Determination of flow through model of W2/500 turbine". (Unpublished).
7	D.G. Ainley & R.A. Jeffs	"Analysis of the air flow through four stages of half vortex blading in an axial compressor". R. & M. No. 2383
8	A.D.S. Carter & E.M. Cohen	"Preliminary investigation of three-dimensional flow through a cascade of aerofoils". P.J. Report No. R.1180. R. & M. 2339.

CIRCULATION

FIG. I.

TURBINE CASING WITH TRAVERSING GEAR IN POSITION.

PITOT / YAWMETER
OF TRAVERSING GEAR.

STATIC PRESSURE
TAPPINGS

PITOT TUBE
& THERMOCOUPLES

YAW CONTROL

RADIAL CONTROL

CIRCUMFERENTIAL
CONTROL

TURBINE NOZZLE
BLADES.
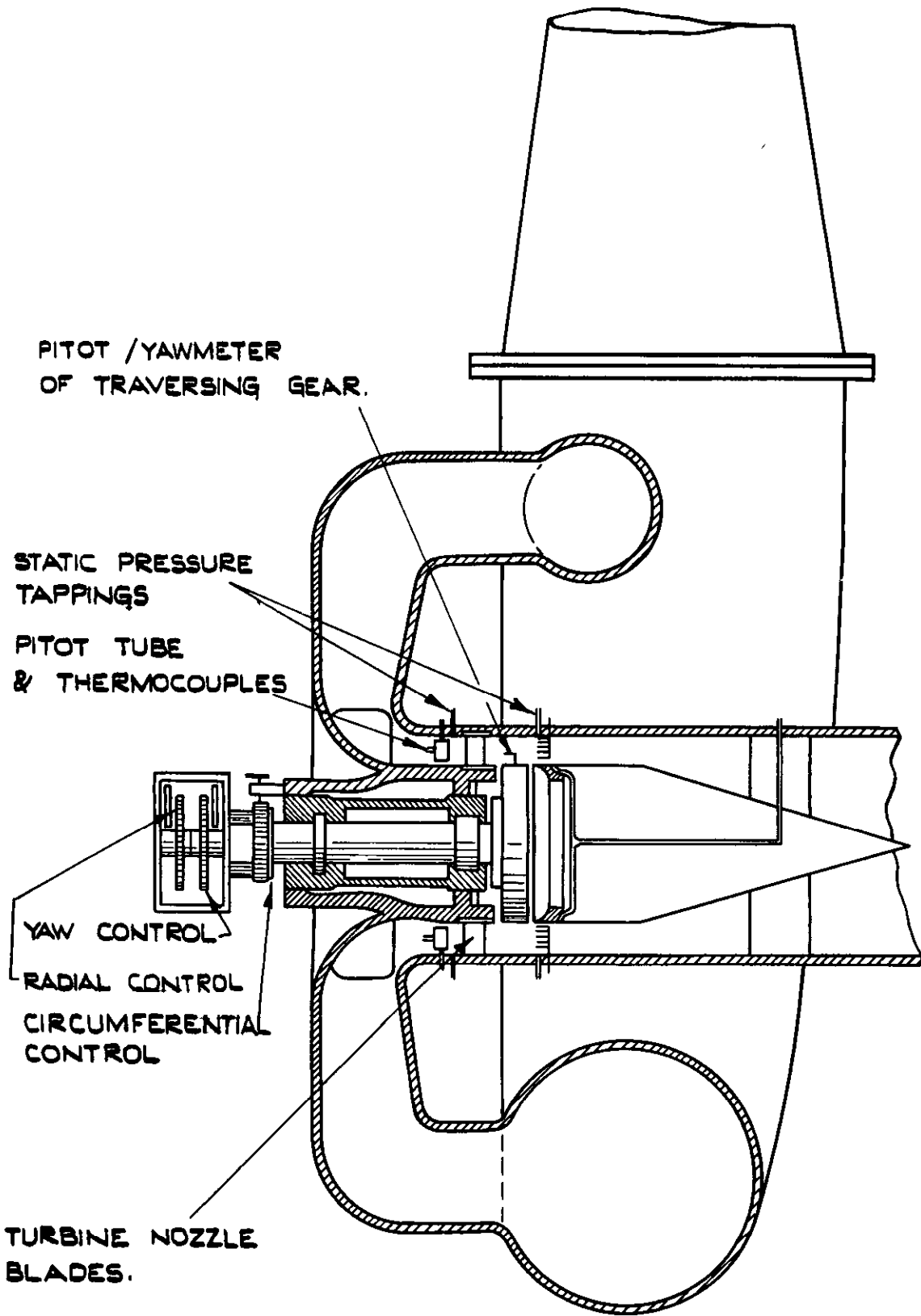
FIG. 2.

NOZZLE BLADE PROFILE.

L.E. RAD. = ·050"

·560"

·625" R.

·185

1·50" RAD.

6·00" RAD.

·876"

·030"

1·00"

FIG. 3.
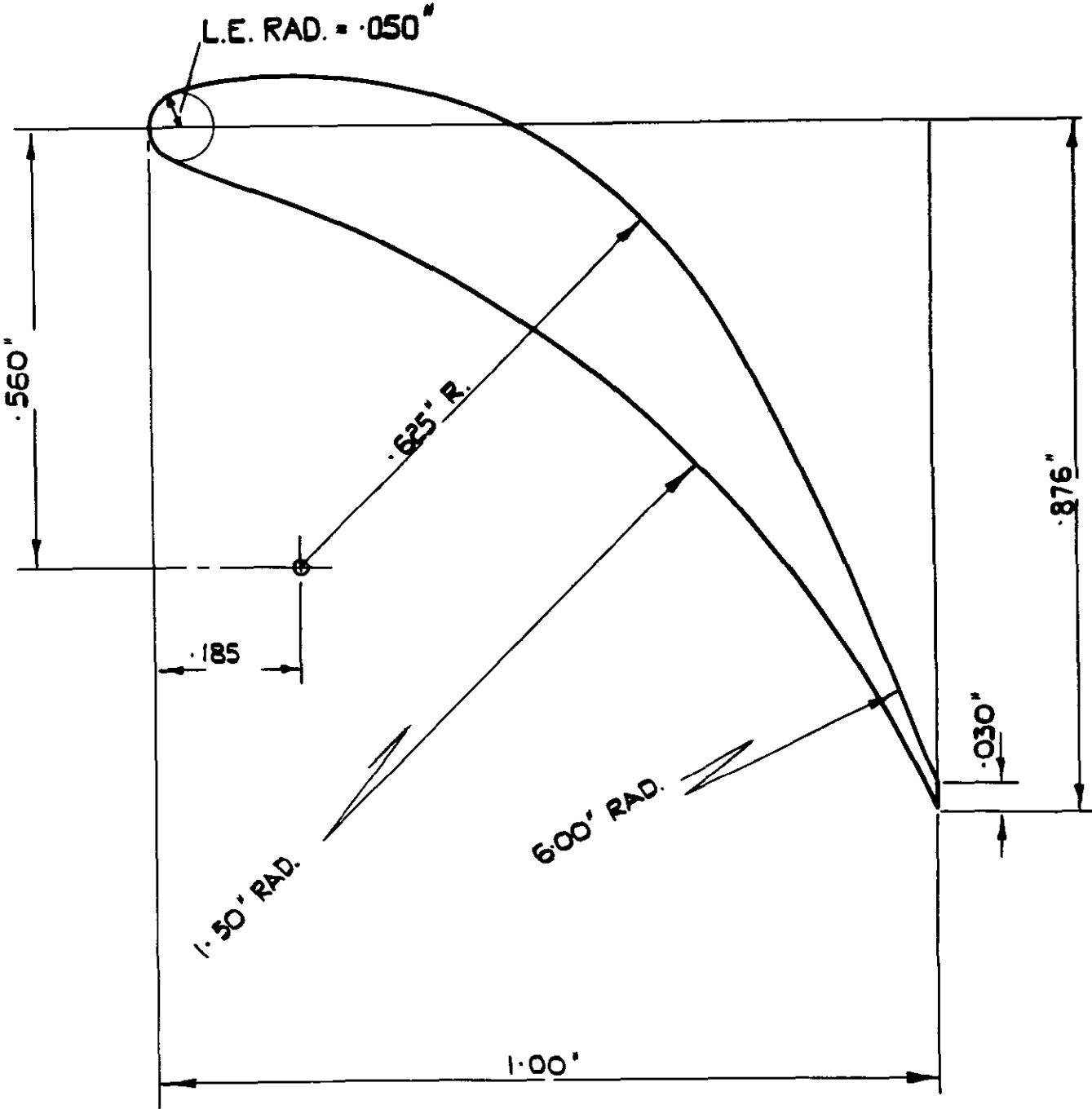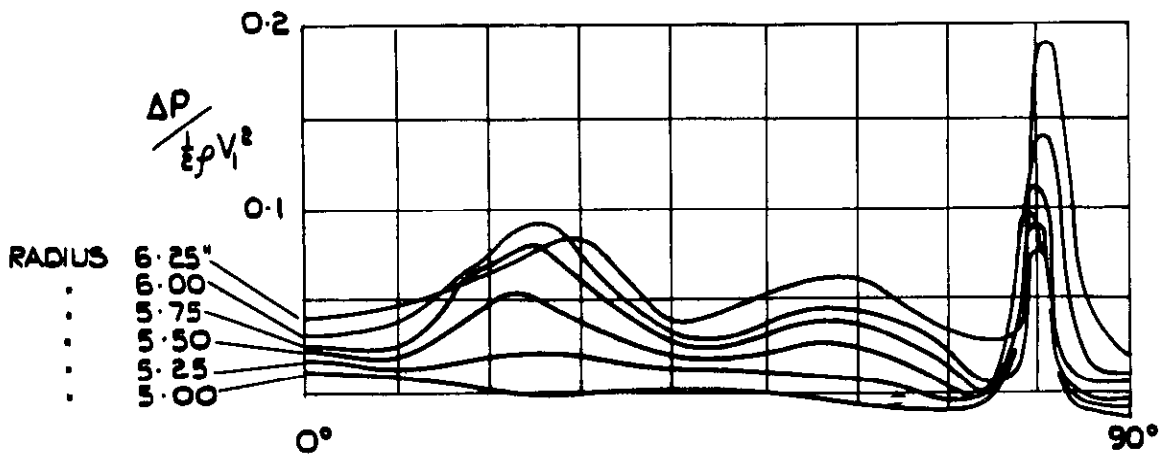
TOTAL HEAD TRAVERSE FOR INLET VOLUTE
OF SINGLE STAGE TURBINE.
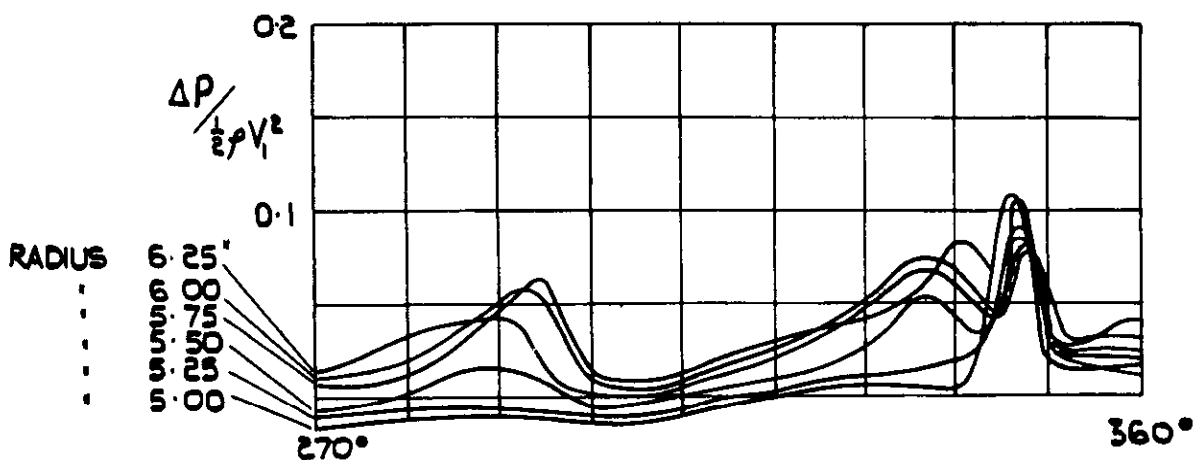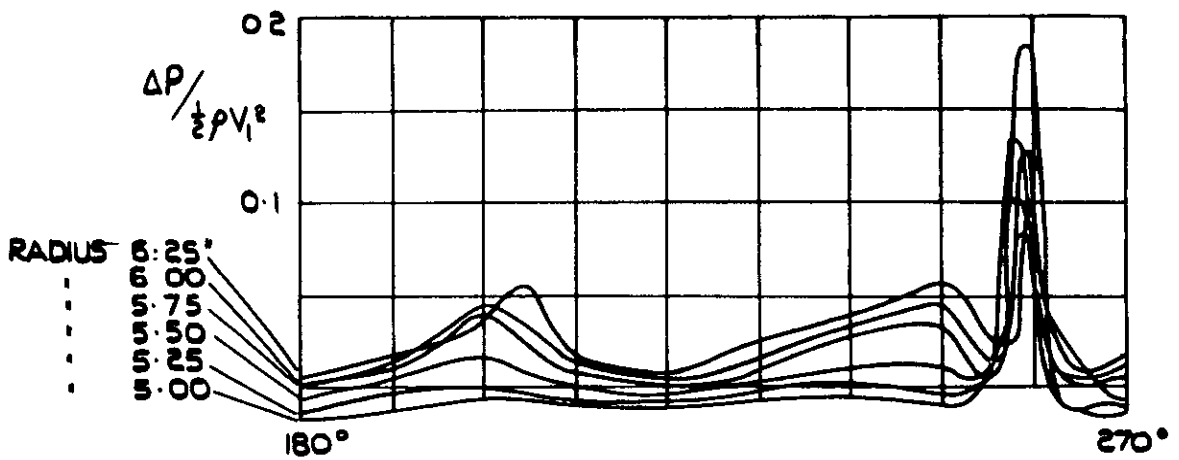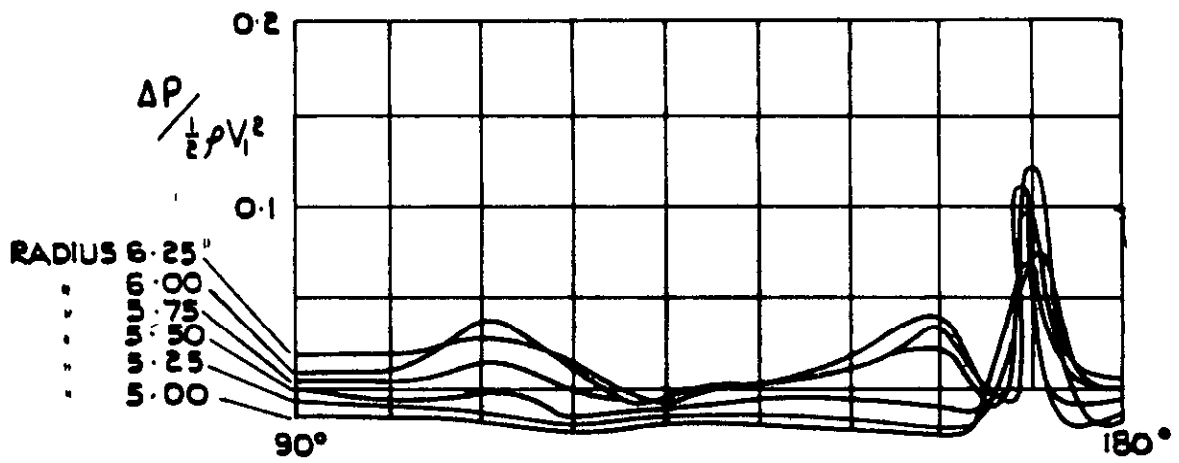
FIG. 4.

DISTRIBUTION OF ABSOLUTE INLET & OUTLET VELOCITIES BEHIND NOZZLES.
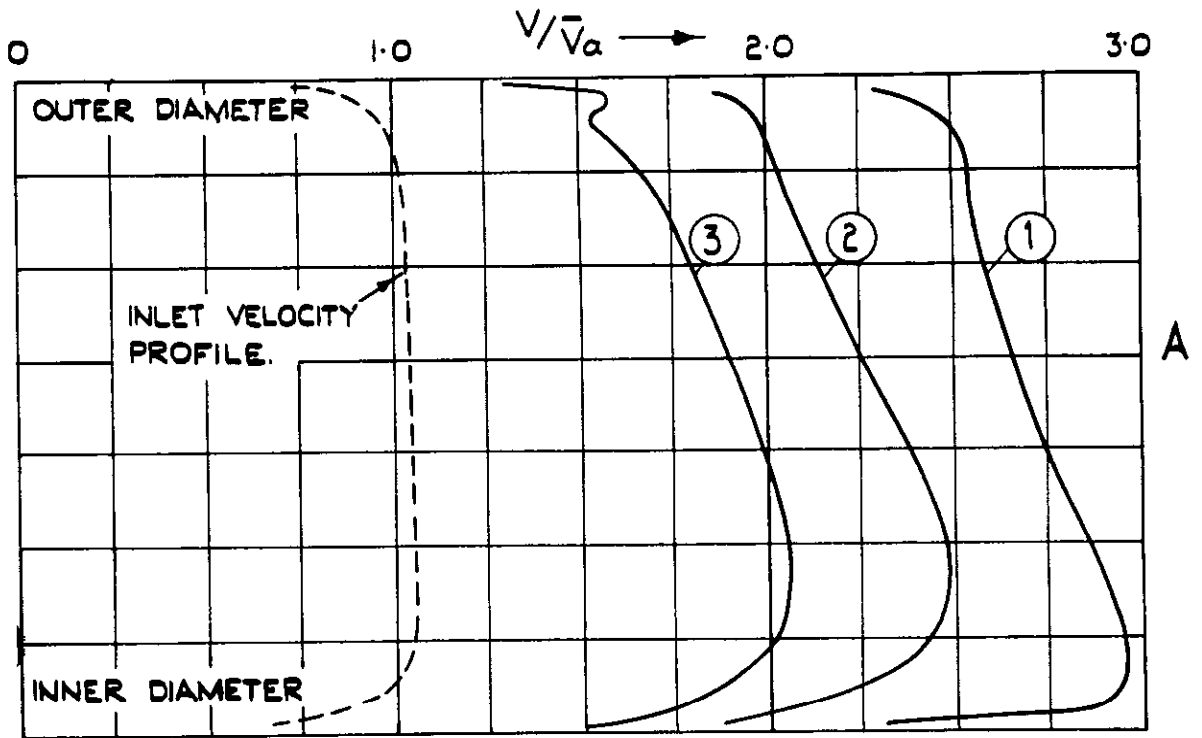
DISTRIBUTION OF AXIAL VELOCITY BEHIND NOZZLES.

——— ACTUAL

----- RADIAL EQUILIB FOR OBSERVED ANGLES

—--— IDEAL FOR $\cos^{-1} \frac{o}{s}$ ANGLES.

FIG. 5.
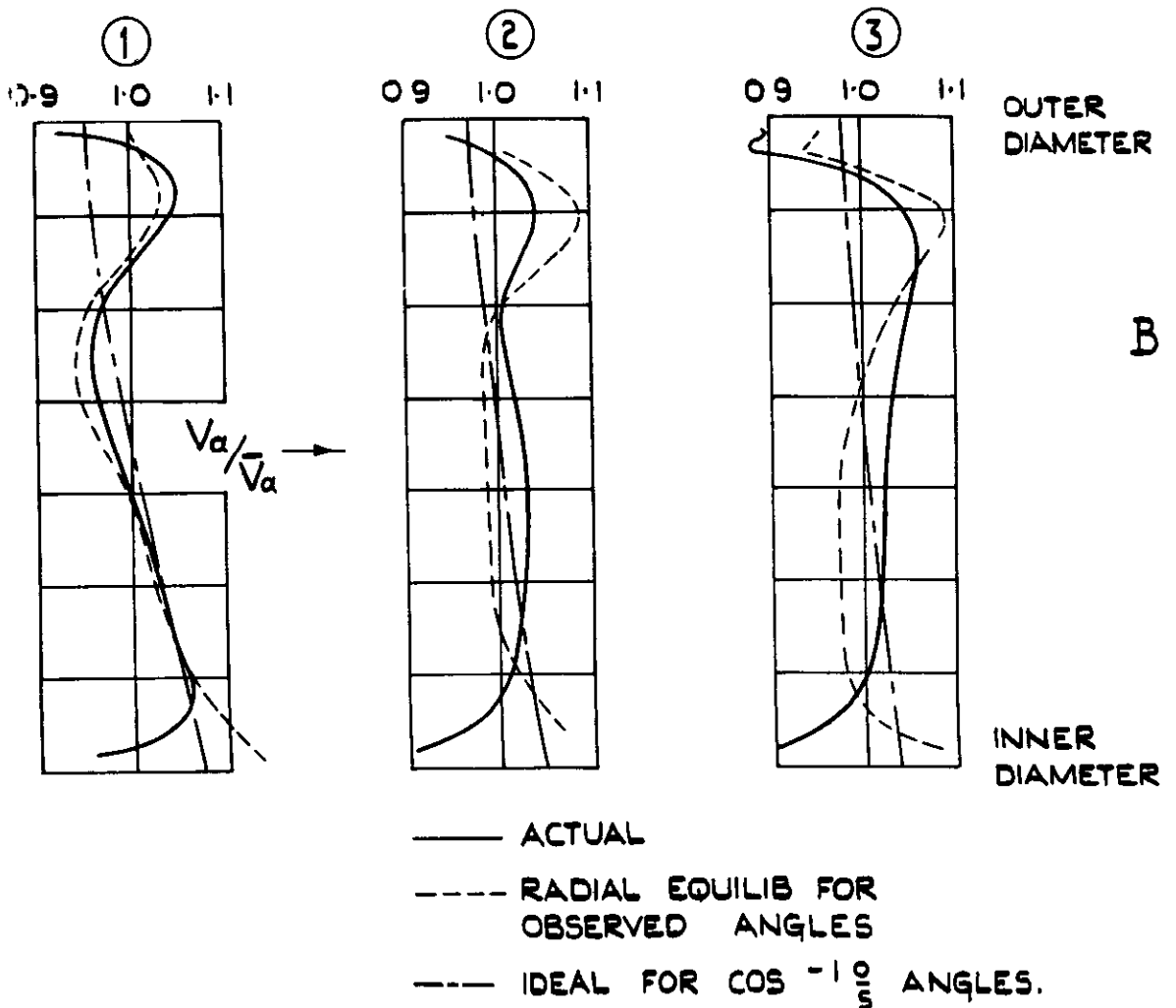
DISTRIBUTION OF WHIRL VELOCITY BEHIND NOZZLES.

A
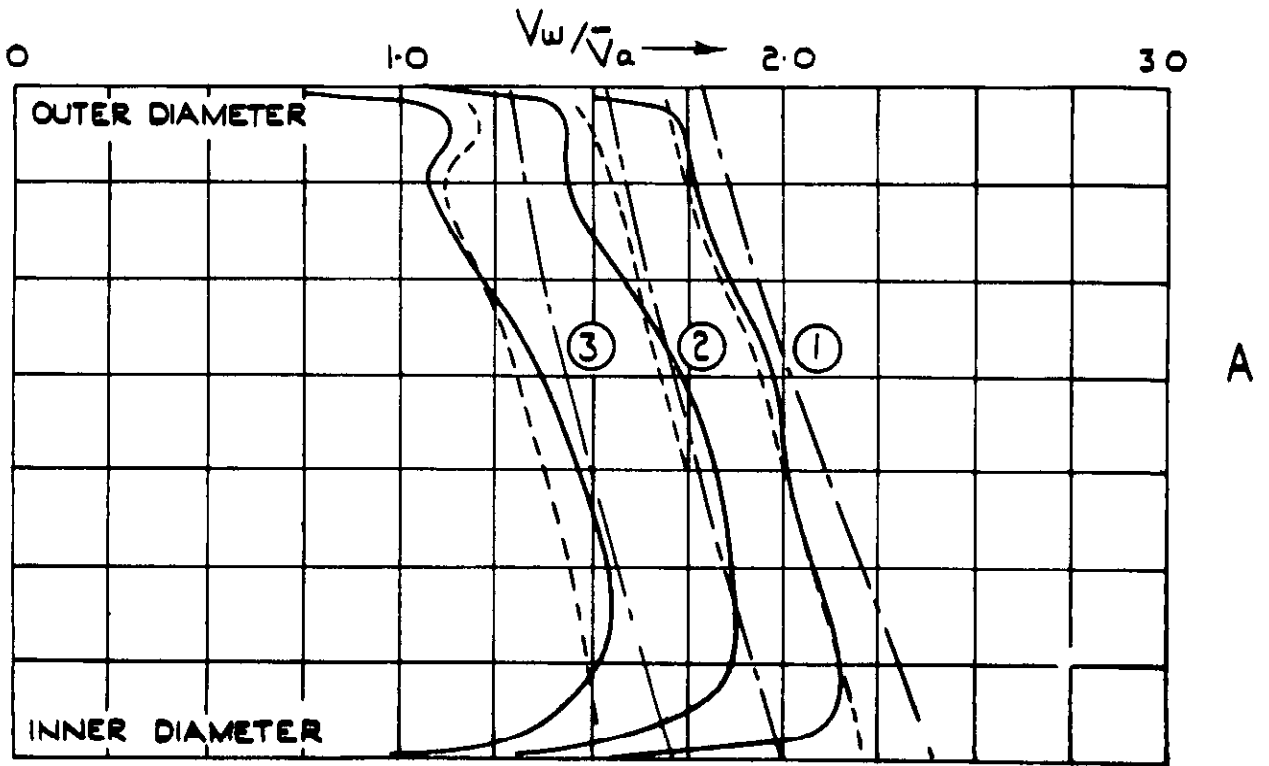
DISTRIBUTION OF GAS OUTLET ANGLE FROM NOZZLES.

B
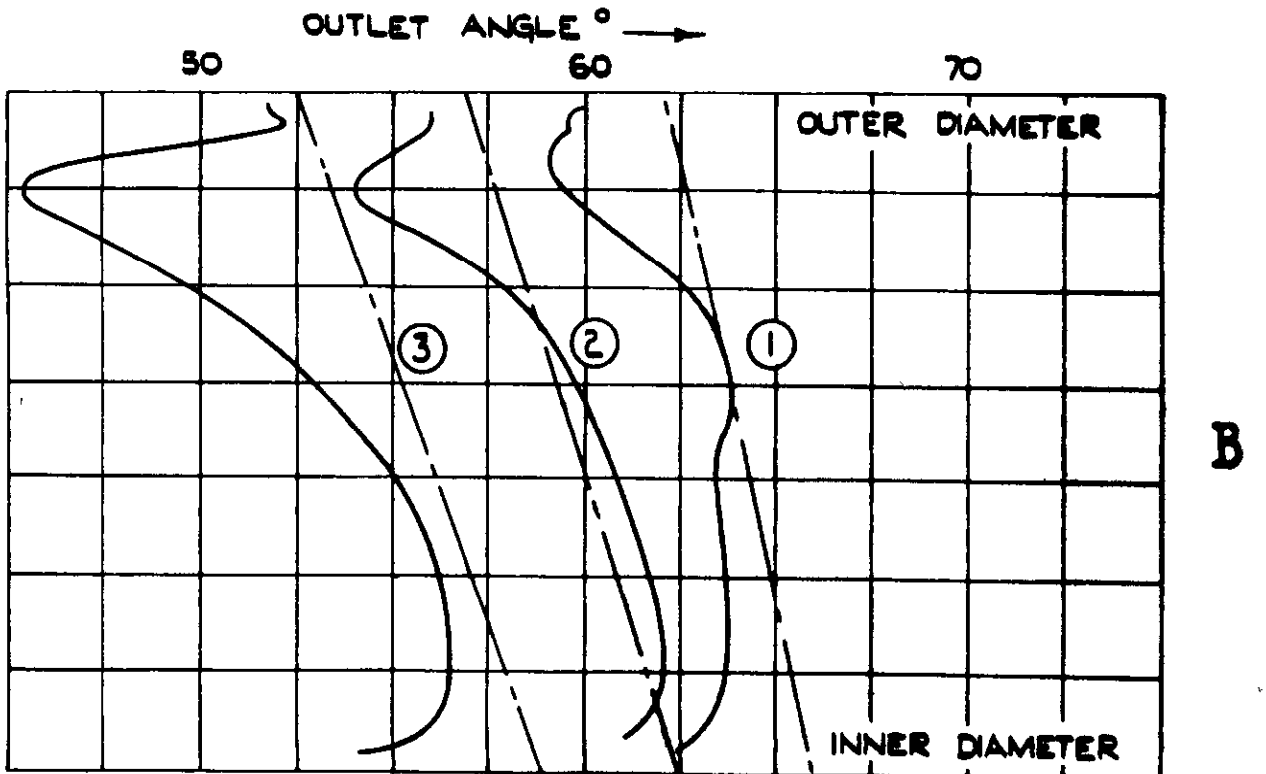
ACTUAL

RADIAL EQUILIBᵐ FOR OBSERVED ANGLES.

IDEAL FOR COS⁻¹ $\frac{o}{5}$ ANGLES.

FIG. 6.

DISTRIBUTION OF TOTAL HEAD LOSS.

$$\Delta P / P_2 - P_2$$

A
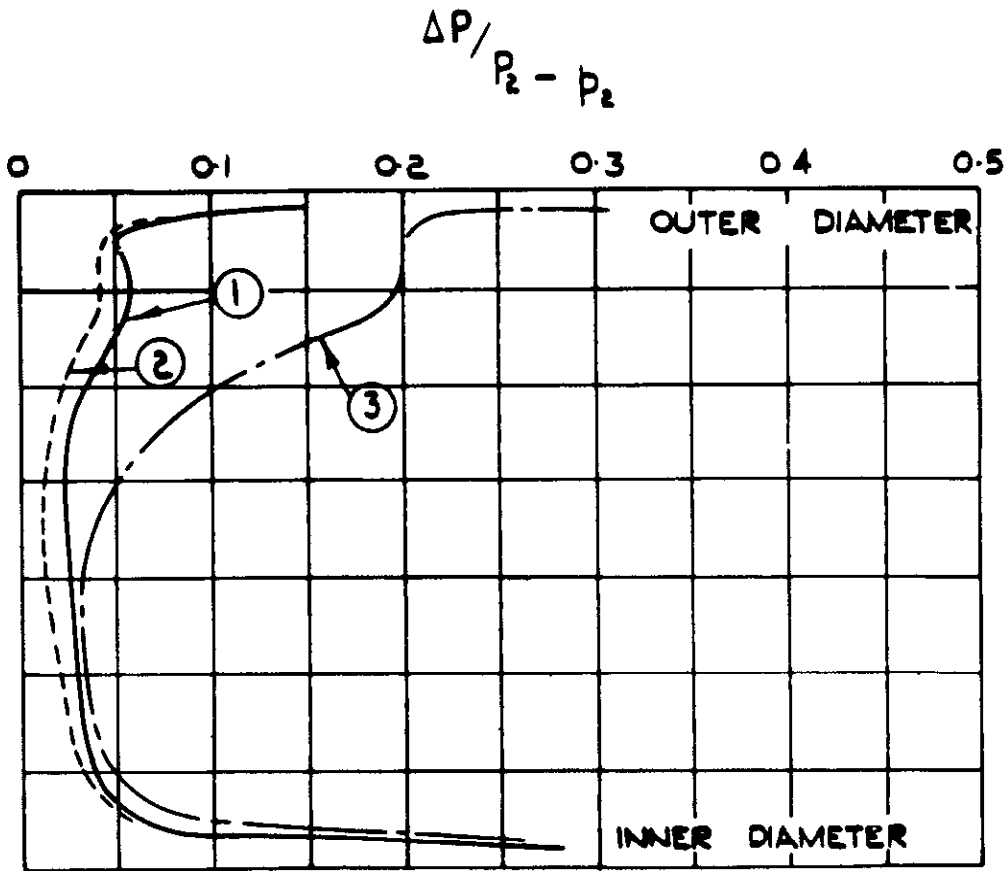
INDUCED EFFECTS ON AIR OUTLET ANGLE.

B

FIG.7.
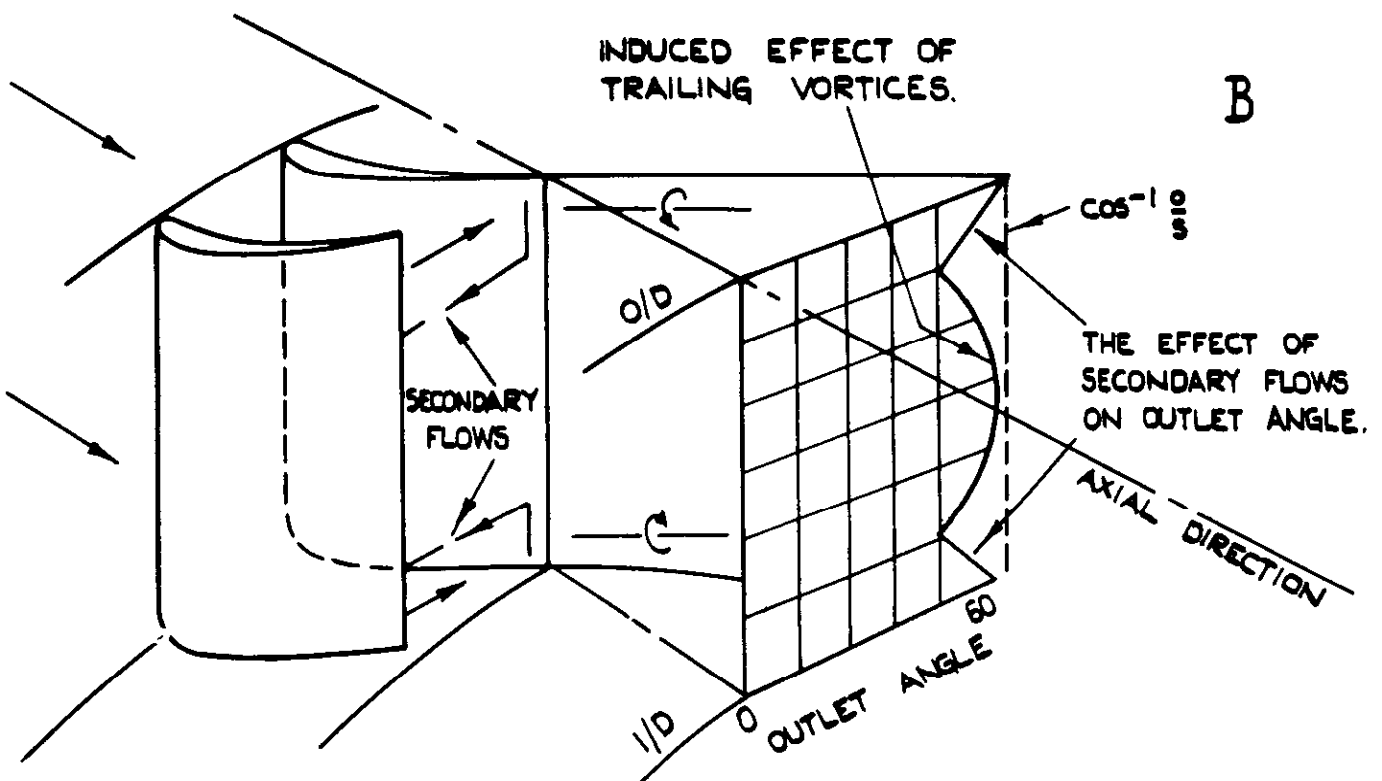
TRAVERSE OF 36-BLADED NOZZLE ROW

SHOWING

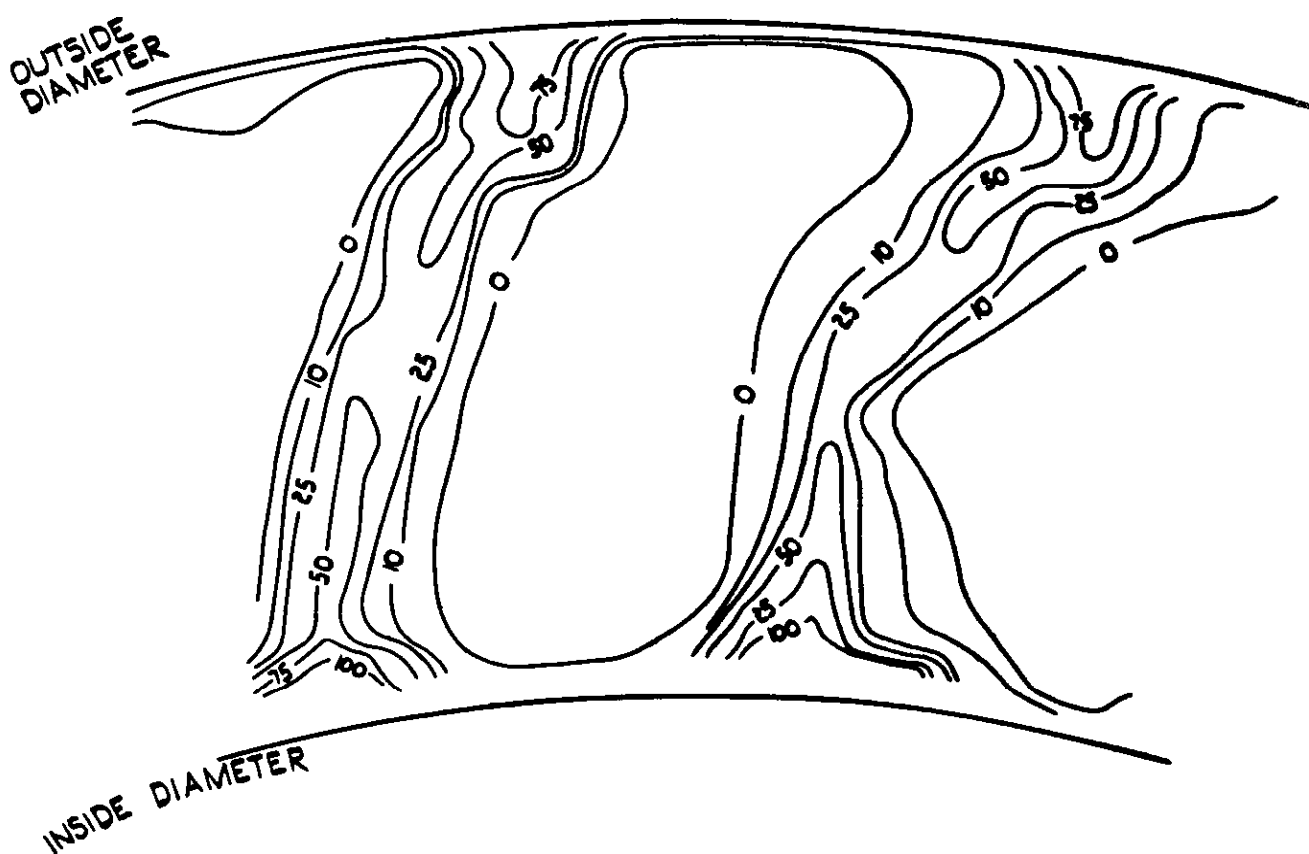## CONTOURS OF $\left(\dfrac{\Delta P}{P_1 - P_{s_1}}\right)$ X 100.
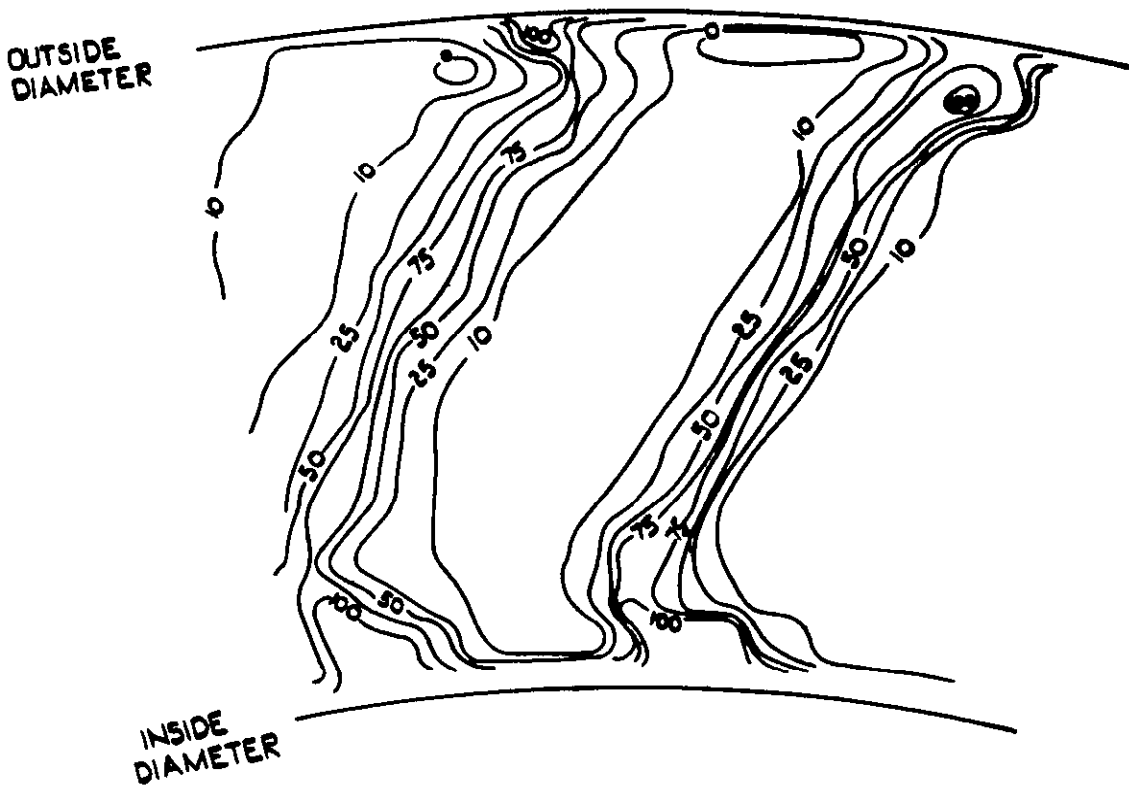
MEAN DIAMETER CONDITIONS :-

DIAMETER	=	11·25"
CHORD	=	1·33"
PITCH/CHORD	=	0·739
OPENING/PITCH	=	0·437
$\cos^{-1}$(OPENING/PITCH)	=	64·10°

FIG. 8.

TRAVERSE OF 27 BLADED NOZZLE ROW

SHOWING

CONTOURS OF $\left(\dfrac{\Delta P}{P_1 - P_{S_1}}\right)$ X 100.

MEAN DIAMETER CONDITIONS

DIAMETER	=	11·25"
CHORD	=	1·33
PITCH/CHORD	=	0·985
OPENING/PITCH	=	0·506
$\cos^{-1}$(OPENING/PITCH)	=	59·60°

FIG. 9.

TRAVERSE OF 22 BLADED NOZZLE ROW

SHOWING

CONTOURS OF $\left(\dfrac{\Delta P}{P_1 - P_{S_1}}\right)$ X 100.

OUTSIDE DIAMETER

INSIDE DIAMETER
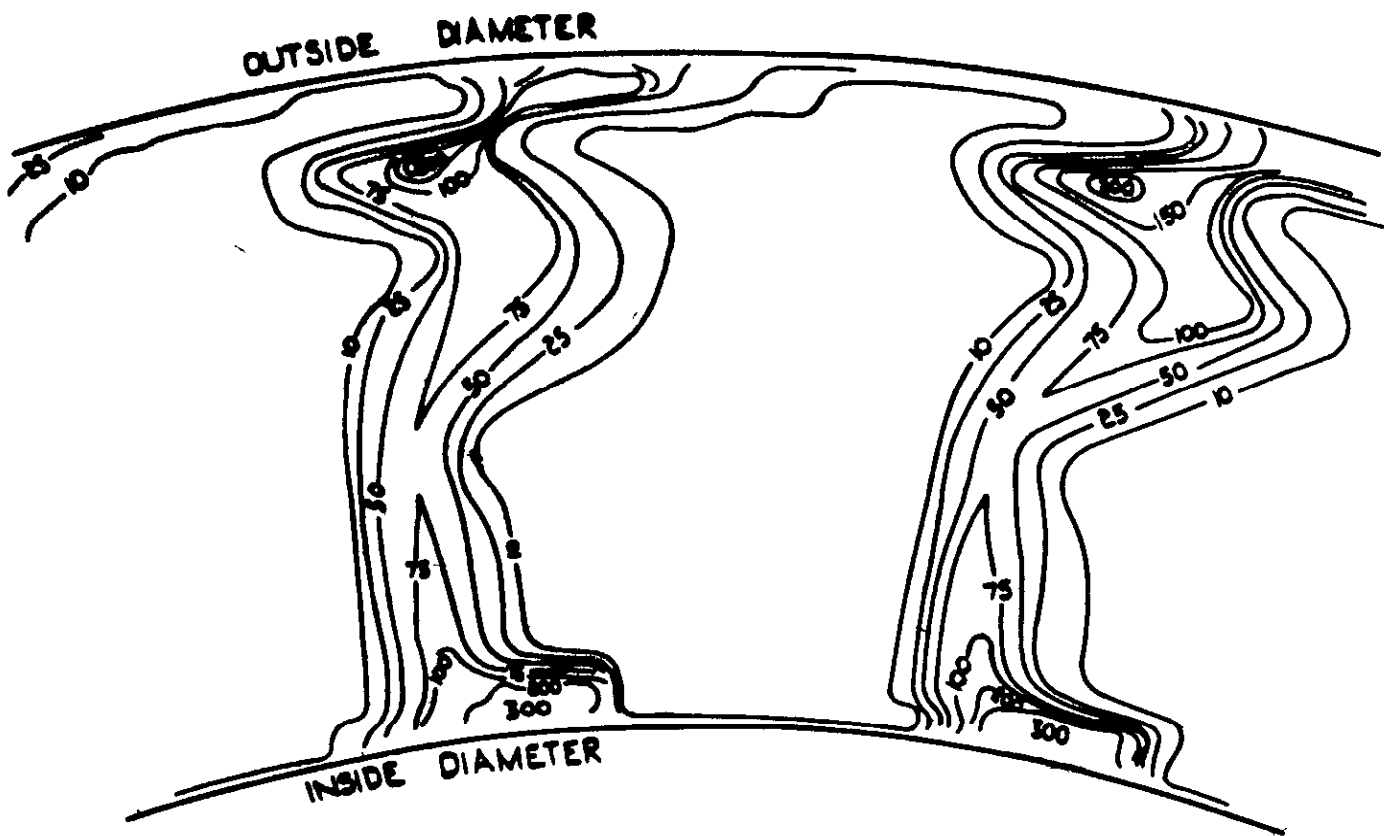
MEAN DIAMETER CONDITIONS.

DIAMETER	:	11·25"
CHORD	:	1·33"
PITCH/CHORD	:	1·208
OPENING/PITCH	:	0·563
$\cos^{-1}$ (OPENING/PITCH)	:	55·70°

LOSS COEFFICIENT V. S/C.

COMPARISON WITH 2-DIMENSIONAL RESULTS.